

Optimized Neural Coding? Control Mechanisms in Large Cortical Networks Implemented by Connectivity Changes

Katy A. Cross,^{1,2*} and Marco Iacoboni^{2,3,4,5,6}

¹Neuroscience Interdepartmental Program, University of California, Los Angeles

²Ahmanson-Lovelace Brain Mapping Center, University of California, Los Angeles

³Department of Psychiatry and Biobehavioral Sciences, University of California, Los Angeles

⁴Semel Institute for Neuroscience and Human Behavior, University of California, Los Angeles

⁵Brain Research Institute, University of California, Los Angeles

⁶David Geffen School of Medicine, University of California, Los Angeles

Abstract: Using functional magnetic resonance imaging, we show that a distributed fronto-parietal visuomotor integration network is recruited to overcome automatic responses to both biological and nonbiological cues. Activity levels in these areas are similar for both cue types. The functional connectivity of this network, however, reveals differential coupling with thalamus and precuneus (biological cues) and extrastriate cortex (nonbiological cues). This suggests that a set of cortical areas equally activated in two tasks may accomplish task goals differently depending on their network interactions. This supports models of brain organization that emphasize efficient coding through changing patterns of integration between regions of specialized function. *Hum Brain Mapp* 00:000–000, 2011. © 2011 Wiley-Liss, Inc.

Key words: imitative behavior; functional MRI; space perception; intention; executive function

INTRODUCTION

Imitation is a ubiquitous behavior, beginning early in infancy [Meltzoff and Moore, 1977] and continuing to play an important role in learning and social interactions throughout life. Work from various fields has converged on the idea that in some circumstances imitation is an automatic phenomenon—it occurs without conscious awareness or volition. Social psychology studies show that people unconsciously imitate during social interactions [Chartrand and Bargh, 1999; Niedenthal et al., 2005]. In addition, some patients with frontal or subcortical lesions exhibit impulsive or reflexive imitation [Brass et al., 2003; De Renzi et al., 1996; Lhermitte et al., 1986]. The release of imitative behaviors after injury not only provides an example of imitation without volition, but also suggests that some active control mechanism normally inhibits automatic imitation.

The neural mechanisms of imitation have been studied in detail [Iacoboni, 2009] and automatic imitation is

Contract grant sponsor: National Center for Research Resources (NCRR); Contract grant numbers: RR12169, RR13642, RR00865; Contract grant sponsors: Brain Mapping Medical Research Organization; Brain Mapping Support Foundation; Pierson-Lovelace Foundation; The Ahmanson Foundation; William M. and Linda R. Dietel Philanthropic Fund at the Northern Piedmont Community Foundation; Tamkin Foundation; Jennifer Jones-Simon Foundation; Contract grant sponsors: Capital Group Companies Charitable Foundation; Robson Family and Northstar Fund; National Institutes of Health (NIH).

*Correspondence to: Katy A. Cross, Ahmanson-Lovelace Brain Mapping Center, 660 Charles E. Young Dr. South, Los Angeles, CA 90095, USA. E-mail: katycross@ucla.edu

Received for publication 14 March 2011; Revised 9 June 2011; Accepted 11 July 2011

DOI: 10.1002/hbm.21428

Published online in Wiley Online Library (wileyonlinelibrary.com).

thought to reflect shared neural mechanisms for action observation and execution [di Pellegrino et al., 1992; Gallese et al., 1996]. However, there is relatively little known about the neural mechanisms involved in controlling automatic imitative tendencies. Although it is plausible that the extensive literature on cognitive control and inhibition of prepotent responses is also applicable to controlling automatic imitation, it has recently been suggested that control over imitative tendencies relies on a distinct inhibitory mechanism [Brass et al., 2009; Spengler et al., 2009]. If this proves true, understanding the control of imitative tendencies may provide insight into neuropsychiatric disorders that are characterized by imitative deficits and social dysfunction, such as autism [Rogers and Williams, 2006; Williams et al., 2006].

At present, the only direct evidence for a unique imitation control mechanism comes from patient and neuroimaging data establishing a dissociation between conflict resolution in imitation interference and Stroop tasks [Brass et al., 2003, 2005]. However, the nature of conflict in these tasks is very different. In the imitation interference task, participants are instructed to perform one of two simple finger movements while a video stimulus displays either the same (congruent) or the opposite (incongruent) action. The appropriate response is either prespecified, with the video serving only as a “go signal,” or specified by a symbolic cue (i.e., “1” for index finger, “2” for middle finger). In both circumstances the action content of the video is irrelevant to successful task performance. Nonetheless, responses are slower when the observed and executed movement conflict, presumably due to an automatic activation of the observed action that has to be controlled to allow the appropriate incongruent response. Thus, increased response time or brain activation on incongruent compared to congruent trials is attributed to the processes required to inhibit the automatic imitative response [Brass et al., 2000, 2001a,b, 2003, 2005].

In the Stroop task, subjects must overcome the automatic tendency to read and instead report the font color of a written word. According to feature overlap models [Kornblum et al., 1990], Stroop conflict results primarily from overlapping stimulus features. This framework is consistent with evidence that resolution of Stroop interference occurs largely at the stimulus rather than response level (i.e., through selective visual attention), [Egner and Hirsch, 2005; Egner et al., 2007; Nee et al., 2007]. In contrast, in the imitation interference paradigms conflict arises from stimulus–response feature overlap. Given evidence for distinct mechanisms involved in stimulus–stimulus, and stimulus–response conflict resolution [Egner et al., 2007], it would not be surprising for control mechanisms to differ for automatic imitation and Stroop tasks even if control of automatic imitation relied on a general response inhibition mechanism.

The aim of the present study is to provide a more definitive test of the hypothesis that overcoming imitative tendencies relies on a specialized imitation control

mechanism by contrasting more similar types of conflict. Spatial compatibility provides an ideal task for comparison because similar to automatic imitation, interference effects stem from stimulus–response overlap. Furthermore, the two tasks can be equated on all dimensions except for the presence or absence of action observation. As such, we employed a spatial compatibility paradigm in which subjects performed one of two finger movements (lifting the index or middle finger of the right hand) in response to either a biological (finger) or nonbiological (dot) dynamic stimulus. For compatible blocks subjects lifted either the same finger as the stimulus (in the case of biological cues) or the finger that corresponded to the location of the moving dot (for nonbiological cues). For incompatible blocks subjects lifted the noncorresponding finger. Automatic activation of the compatible response occurs regardless of whether participants are instructed to respond with a compatible or incompatible mapping, even for a nonbiological stimulus [Eimer et al., 1995; Stürmer and Leuthold, 2003]. As a result, automatic activation of the compatible response must be controlled in order to perform the incompatible mapping. Thus, if a distinct imitation control mechanism exists [Brass et al., 2005, 2009], we would expect to observe a dissociation for biological and nonbiological stimuli, even under these highly similar task demands. To test this hypothesis, we examined brain regions that are more active for incompatible than compatible trials for each cue type. These activations could then be directly compared between cue types to examine areas of overlap as well as differences in regional brain activity.

In addition to examining differences in levels of brain activity for compatible and incompatible trials, we also measured changes in functional connectivity using a psychophysiological interaction analysis (PPI). This method reveals brain regions in which functional connectivity with a seed region is modulated by task condition [Friston et al., 1997], reflecting cognitively relevant changes in network interactions. The goal of this analysis was twofold. First, the particular role of a region or a network may differ depending on the nature of its interactions with different regions or networks [Friston, 2002; Stephan et al., 2004], such that a single region may have similar activation magnitudes in two different tasks, but different patterns of functional connectivity with other brain regions [Garraux et al., 2005]. Second, previous studies have used a similar strategy to examine potential targets of top-down control in a wide variety of tasks [Banks et al., 2007; Egner and Hirsch, 2005; Wolbers et al., 2006]. This strategy is based on the idea that sources of control would show increased connectivity with target regions in contexts requiring control (i.e., during incompatible trials) compared to those not requiring control (i.e., during compatible trials). As such if the targets of control are distinct when conflict arises from biological and nonbiological cues, we would expect different patterns of compatibility-modulated functional connectivity.

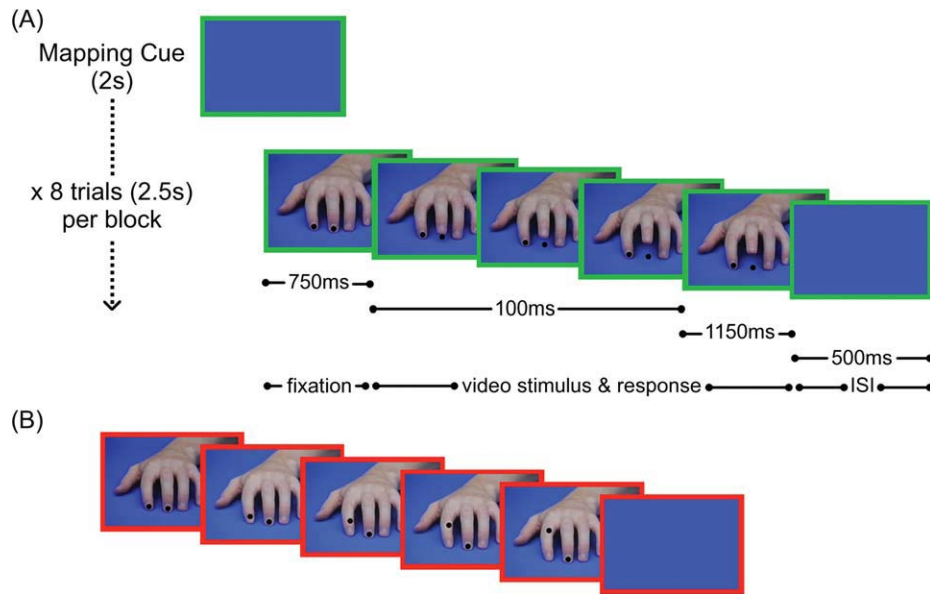


Figure 1.

Behavioral paradigm. **(A)** Example of block structure (imitate compatible block). **(B)** Example of spatial incompatible trial. Border color denotes task instructions for 2 s at the onset of and throughout each block (green = compatible; red = incompatible). [Color figure can be viewed in the online issue, which is available at wileyonlinelibrary.com.]

METHODS

Participants

Twenty-eight adult participants were recruited from the UCLA and surrounding community through advertisements in the university newspaper and free online bulletins. Four subjects were excluded from analysis due to scanner equipment technical failure (one subject) and failure to meet inclusion criteria discovered after enrollment (three subjects). The remaining 24 participants (12 female) were 18–33 years old (mean = 22.4, standard deviation = 3.5), right-handed, had normal or corrected-to-normal vision and reported no history of neurologic or psychiatric disorders and no current use of psychoactive medication. The study was approved by the UCLA Institutional Review Board. Written informed consent was obtained from all subjects and subjects were paid \$25 per hour for participating.

Behavioral Paradigm

We used a choice response task to compare imitation and spatial compatibility during fMRI. Video stimuli consisted of five frames. The first frame was always the same, showing a left hand resting on a surface in a relaxed position with the palm down and fingers facing the subject, as in previous studies [Brass et al., 2000; Iacoboni et al., 1999, 2001; Koski et al., 2003]. Two black dots were superimposed over the index and middle fingernails. After 750 ms, the video depicted upward movement (four frames shown at a

rate of 34 ms per frame) of either a finger or a dot. In imitative trials, the index or middle finger was extended, moving upward from the resting position, while the dots remained stationary; in spatial trials, one of the dots moved upward while the fingers remained stationary. The trajectory of the finger and dot movements was identical, such that the primary difference between imitation and spatial trials was the presence or absence of biological motion. The final frame remained on the screen for 900 ms, providing the response window. Trials were separated by a 500-ms interstimulus interval (ISI) consisting of a blank blue background.

Subjects were instructed to extend their own index or middle finger in response to the videos, releasing one of two buttons that were depressed whenever they were not responding. The color of a border outlining the video stimuli indicated the response instructions. For half of all blocks, a green border designated that subjects should lift the finger on the same side as the video (i.e., index finger in response to index finger extension, or to upward motion of dot over index finger). These represented the compatible blocks. For the other half of the blocks, a red border indicated that subjects should lift the finger on the opposite side as the video (i.e., index finger in response to middle finger extension, or to upward motion of dot over middle finger). These represented the incompatible blocks. The result was a 2 (cue type: imitation, spatial) × 2 (compatibility: compatible, incompatible) design consisting of a total of four conditions (see Fig. 1).

Task blocks were preceded by a 2-s mapping cue (blank blue background with red or green border), giving subjects

time to process the instructions before beginning the block. The mapping cue was followed by eight 2.5-s trials comprising a 20-s task block. Task blocks alternated with 20-s rest blocks (blank blue screen, no border). The stimulus–response mapping rule (compatible, incompatible) was alternated every two blocks (to minimize the frequency of task set changes and maximize compatibility effects without losing too much power to low-frequency drift) and the cue type alternated every block. Four possible stimulus orders were created in these constraints, each beginning with a different condition. Each subject performed all four possible orders (in four runs), with the order of runs counterbalanced across subjects.

Procedure

Immediately prior to scanning, each subject was familiarized with the task during a brief practice session. Subjects subsequently performed a total of eight blocks of each of the four conditions [spatial compatible (SpC), spatial incompatible (SpI), imitation compatible (ImC), imitation incompatible (ImI)] during fMRI scanning. The session was divided into four runs each 5:56 min long, between which the subjects were allowed a short break. Each run was preceded by a reminder of the instructions.

MRI Data Acquisition and Processing

Images were acquired on a Siemens (Erlangen, Germany) 3T Trio MRI scanner. For functional runs we acquired 178 T2*-weighted echoplanar images (EPIs) [repetition time (TR) 2,000 ms; echo time (TE) 28 ms; flip angle = 90°; 34 slices; slice thickness 4 mm; matrix 64 × 64; FOV 192 mm]. To allow for T1 equilibrium the first two volumes of each functional scan are automatically discarded before data collection begins. Two sets of structural images were also acquired for registration of functional data: a T2-weighted matched-bandwidth high-resolution scan with the same slice prescription as the EPI [repetition time (TR) 5,000 ms; echo time (TE) 34 ms; flip angle = 90°; 34 slices; slice thickness 4 mm; matrix 128 × 128; FOV 192 mm]; and a T1 weighted magnetization prepared rapid-acquisition gradient echo image (MPRAGE) [TR, 1,900 ms; TE 2.26 ms; flip angle = 9°; 176 sagittal slices; slice thickness 1 mm; matrix 256 × 256; FOV 250 mm]. Visual stimuli were timed and presented with Presentation software (Neurobehavioral Systems, Albany, CA) through magnet-compatible LCD goggles. Responses were recorded with a magnet-compatible response box (Current Designs, Philadelphia, PA).

Image preprocessing and data analysis were performed with FSL version 4.1.4 (Centre for Functional Magnetic Resonance Imaging of the Brain software library, www.fmrib.ox.ac.uk/fsl) [Smith et al., 2004]. Images were realigned to the middle volume to compensate for any head motion using MCFLIRT [Jenkinson et al., 2002]. Images were then examined visually for gross motion

artifacts that cannot be corrected for with simple realignment. When motion artifacts were detected, a nuisance regressor for each affected volume (mean = 2 vols/run, SD = 3.6) was included in the general linear model. In addition one run for each of two subjects was excluded for excessive motion (>10% volumes exhibiting motion artifacts). Data were temporally filtered with a high-pass filter cutoff of 100 s and spatially smoothed with a 6-mm full width half maximum Gaussian kernel in three dimensions.

Task Activation Analysis

Statistical analyses were performed at the single subject level using a general linear model (GLM) with fMRI Expert Analysis Tool (FEAT). After convolution with a canonical double-gamma hemodynamic response function, each block type (ImC, ImI, SpC, SpI) was included as a regressor in the GLM. In addition, the mapping cue beginning each block and the reaction time for each trial (orthogonalized with respect to EVs of interest) were included in the model as nuisance regressors. Temporal derivatives were included for each regressor to account for variability in the hemodynamic response. Contrasts estimated included incompatible–compatible for both spatial and imitation (ImI – ImC and SpI – SpC) as well as the interaction between cue type and compatibility [(ImI – ImC) – (SpI – SpC) and (SpI – SpC) – (ImI – ImC)]. In addition we computed cue type main effect [(ImI + ImC) – (SpI + SpC) and (SpI + SpC) – (ImI + ImC)].

First level contrast estimates were computed for each run and then registered to standard space (Montreal Neurological Institute, MNI) in three stages. The middle volume of each run of individual EPI data was registered first to the coplanar matched-bandwidth high-resolution T2-weighted image and subsequently, the coplanar volume was registered to the T1-weighted MPRAGE. Both of these steps were carried out using FLIRT (affine transformations: EPI to co-planar, 3 degrees of freedom; co-planar to MPRAGE, 6 degrees of freedom) [Jenkinson et al., 2002]. Finally registration of the MPRAGE to MNI space (FSL's MNI Avg152, T1 2 × 2 × 2 mm³) was carried out with FLIRT (affine transformation, 12 degrees of freedom) and refined using FNIRT (nonlinear transformation) [Jenkinson and Smith, 2001; Jenkinson et al., 2002].

Contrast estimates for each subject were then computed treating each run as a fixed effect. Finally, a group level analysis was performed to calculate a group mean for each contrast treating each subject as a random effect using FSL's FLAME (FMRIB's local analysis of mixed effects) Stages 1 and 2 [Beckmann et al., 2003; Woolrich, 2008; Woolrich et al., 2004]. Group images were thresholded at $z > 3.1$ ($P < 0.001$), corrected for multiple comparisons using cluster-based Gaussian random field theory controlling family-wise error across the whole-brain at $P < 0.05$. Common areas of activation for spatial and imitative cues were examined with a simple conjunction overlay

analysis, which includes all areas that show significant activation for Incompatible > Compatible ($z > 3.1$, corrected) for both spatial and imitative cues.

Functional Connectivity Analysis

In addition to the typical subtraction analysis described above, we carried out a psychophysical interaction analysis [PPI; Friston et al., 1997] examining context-dependent changes in functional connectivity. As described in the Results section, a similar set of sensorimotor regions was activated more for incompatible compared to compatible mapping for the two cue types. To determine whether these areas had distinct patterns of functional connectivity (as would be expected for dissociable imitation and spatial mechanisms), we carried out analyses examining differences in sensorimotor network functional connectivity for incompatible versus compatible blocks. This was done independently for spatial cues and for imitative cues and then directly compared.

The PPI analysis was carried out using eight cortical seeds obtained from the sensorimotor network revealed by the Incompatible > Compatible contrasts (see Results). Functional seeds were created in standard (MNI) space using the conjunction overlay of $Spl > SpC$ and $ImI > ImC$, both thresholded at $z > 3.1$ (corrected for multiple comparisons; Fig. 2A). For each seed we carried out a separate PPI analysis for spatial cues and imitative cues according to the following procedure: The seed was warped back into individual subject space, and the mean temporally filtered time series of the voxels within the seed was extracted for each run performed by each subject. No other processing was applied to the extracted timecourse, so that it reflected the mean temporally filtered raw signal from the seed voxels. A PPI regressor was computed as the product of the mean-corrected seed activation (“physiological regressor”) and a vector coding for the differential effect of compatibility ($SpI-SpC$ for the spatial PPI, $ImI-ImC$ for the imitation PPI; “psychological regressor”). In addition to the PPI regressor, regressors for the task effects (as described above) as well as the temporally filtered time series from the seed region were also included in the model. This ensures that PPI estimates reflect the compatibility induced differences in covariation between brain regions above and beyond that explained by shared task input or task-independent functional connectivity (i.e., due to anatomical connections, etc.). Thus, PPI results should reflect regions that show significantly different covariation (i.e., functional connectivity) with the seed region for compatible vs. incompatible blocks.

Imitation and spatial PPI contrast estimates for each run were entered into a fixed effects model for each subject to compute PPI estimates for each cue type as well as the difference between cue types. These results were entered into a group analysis using treating subjects as random effects. Comparison of PPI effects between cue types was

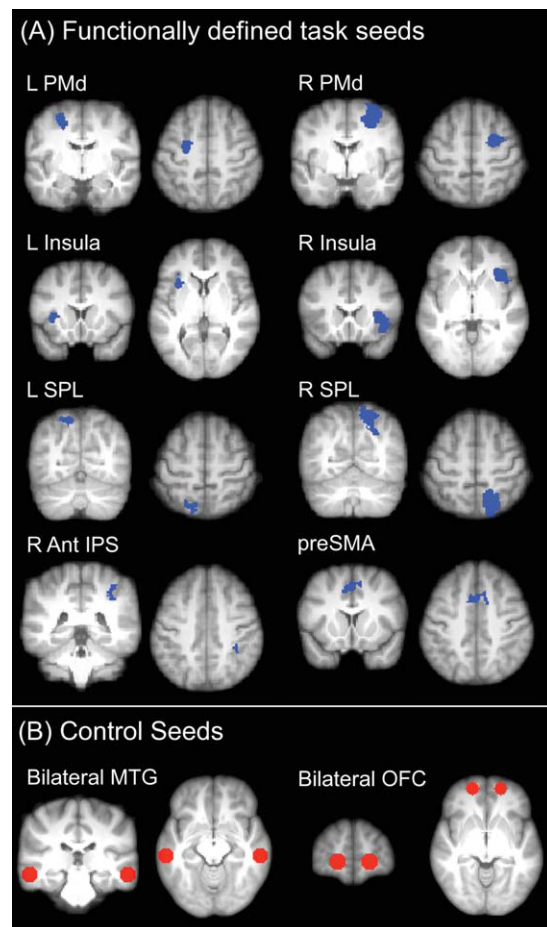


Figure 2.

PPI Seeds. **(A)** Eight seeds obtained from conjunction overlay of $Spl > SpC$ and $ImI > ImC$. R = right; L = left; SPL = superior parietal lobe; PMd = dorsal premotor; SMA = supplementary motor area; ACC = anterior cingulate cortex. **(B)** Four task-unrelated control seeds. [Color figure can be viewed in the online issue, which is available at wileyonlinelibrary.com.]

restricted to only those areas in which compatibility-modulated functional connectivity was significant in the individual cue type analyses, using an inclusive mask from the results of PPI analyses for both cue types.

The product is a separate set of PPI results for each seed, showing the regions with compatibility modulated functional connectivity to the seed region during imitative and spatial blocks, as well as regions in which this compatibility modulated functional connectivity was different for the two cue types. Examination of these results showed surprisingly similar patterns of connectivity changes in all eight seeds. Therefore, in order to simplify the results and achieve more power, we averaged over the eight seed PPIs for each subject (treating seeds as fixed effects) to examine shared connectivity with the entire set of seed regions (henceforth referred to as the “network seed”).

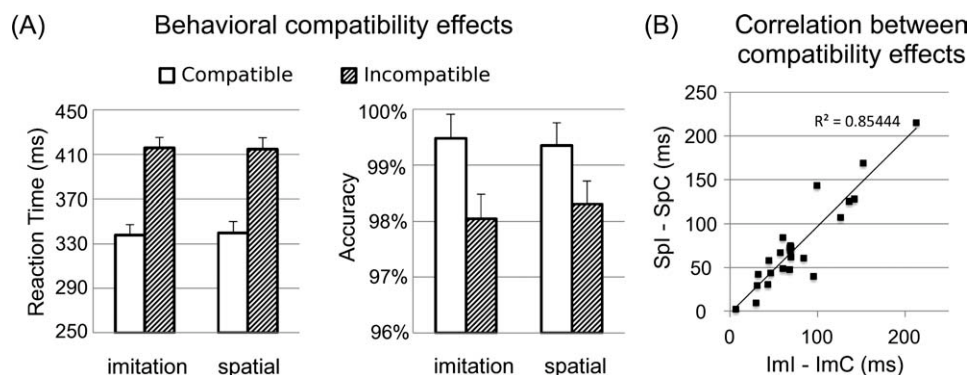


Figure 3.

Behavioral results. **(A)** Reaction time (left) and accuracy (right) data for all four conditions. **(B)** Scatterplot showing reaction time compatibility effects for imitative (x axis) and spatial (y axis) cue types.

Several post-hoc analyses were performed to further examine regions showing differential PPI results for spatial and imitative cues. The first aimed to clarify what was driving the compatibility modulated functional connectivity. For example, differences between functional connectivity during compatible and incompatible blocks could be due to increased functional connectivity in one condition, decreased functional connectivity in the opposite condition, or both. To disentangle these contributions, PPI analyses comparing each condition to baseline were performed as described above, changing only the psychological regressor. That is, instead of comparing functional connectivity for incompatible and compatible blocks using psychological regressors ImI-ImC and SpI-SpC, changes in functional connectivity between each condition and baseline (BL) were examined using the psychological regressors ImC-BL, ImI-BL, SpC-BL, and SpI-BL. Parameter estimates from each subject were extracted for the regions showing significant PPI effects in the compatibility PPI analysis using FSL's Featquery.

The second post-hoc analysis aimed to further explore activation magnitudes in regions with significant PPI effects. The regions emerging from the connectivity analyses did not show different levels of activation for compatible and incompatible blocks in the task activation analysis. This would suggest that in these regions the functional connectivity with the compatibility modulated network, but not magnitude of activation is modulated by compatibility. To determine whether this was in fact the case or whether the failure to detect compatibility effects in these regions was instead a result of insufficient sensitivity we performed an ROI analysis. For each region showing significantly different PPI effects (indicating significant compatibility-modulated functional connectivity) between the two cue types we extracted parameter estimates of the magnitude of activation for each condition compared to baseline and performed a Cue Type (imitation, spatial) × Compatibility (compatible, incompatible) ANOVA.

Finally, to ensure that the striking similarity between task-induced functional connectivity with each of the visuomotor network seeds was not a result of some unidentified task-independent factor, we chose four additional seeds that were not modulated by the task and performed the same stream of analyses. The seeds were bilateral middle temporal gyrus ($\pm 58, -28, -12$) and bilateral frontal pole ($\pm 18, 56, -2$) (Fig. 2B), chosen to be outside areas activated for the Task > Rest contrast. Spheres of radius 9 mm (volume = 3,054 mm³) centered on the above coordinates were used so that the volume was similar to the average volume of the functionally defined seeds (mean = 3,102 mm³, SD = 2,886).

RESULTS

Behavioral Data

Mean reaction time (RT) was calculated for correct responses in each condition. Trials with RT greater than two standard deviations from the mean were considered outliers and excluded from analysis (0.6–3.4% of trials for each subject). Reaction time analysis was carried out using a cue type (spatial, imitation) × compatibility (compatible, incompatible) repeated measures ANOVA. This revealed only a main effect of compatibility [$F(1,23) = 61.7, P < 0.001$], indicating that responses on incompatible trials (mean = 415 ms, SD = 67.4 ms) were slower than compatible trials (mean = 338 ms, SD = 36.2 ms) regardless of the cue type. Accuracy data showed an identical pattern when subjected to the same ANOVA, with a small but significant main effect of compatibility [$F(1,23) = 21.7, P < 0.001$]; compatible: mean = 99.4%, SD = 0.9%; incompatible: mean = 98.2%, SD = 1.9%] (Fig. 3A).

In addition, we computed a correlation between compatibility effects (incompatible – compatible reaction time) for the two cue types. If similar cognitive and neural mechanisms are involved for spatial and imitative cues, one

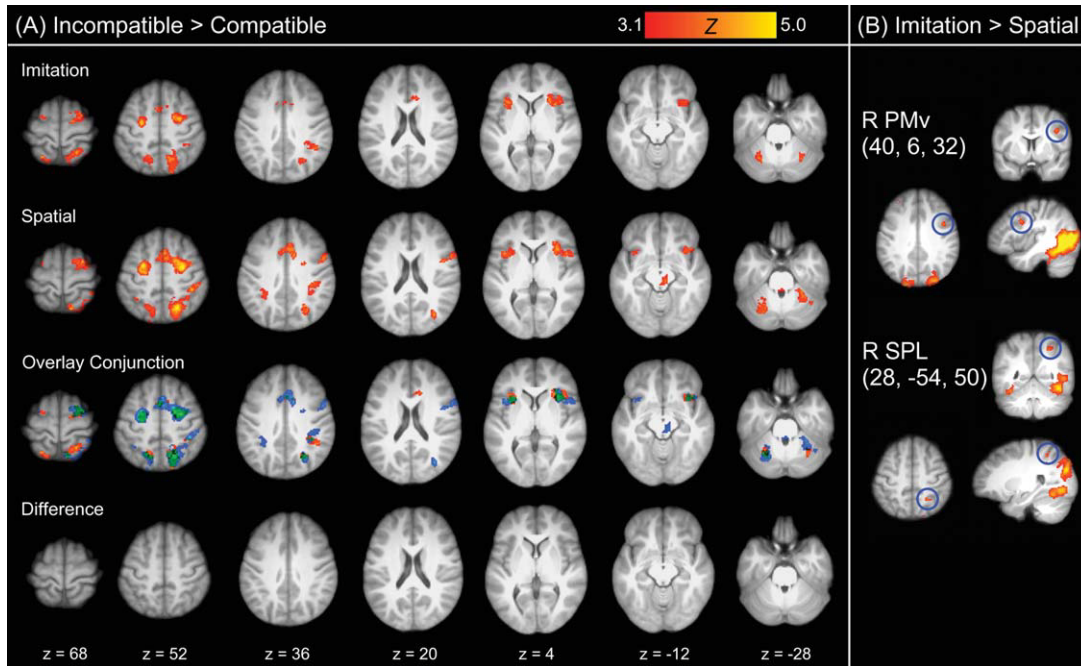


Figure 4.

Activation analysis results. **(A)** Incompatible > Compatible contrasts for imitative (1st row) and spatial (2nd row) cues are very similar. Conjunction overlay of imitation and spatial results (3rd row) illustrate significant overlap. Orange = imitation; blue = spatial; green = overlap. Difference of imitation and spatial cues (4th row) depicts lack of cue \times compatibility interaction (even when threshold is lowered to $z > 1.7$, corrected). Maps are

thresholded at $Z > 3.1$, corrected. **(B)** Imitation > Spatial contrast (collapsed across cue type), depicting activation in fronto-parietal areas previously associated with imitation. L = left; R = right; coordinates are in MNI space; PMv = ventral premotor cortex; SPL = superior parietal lobe. Maps are thresholded at $Z > 3.1$, uncorrected.

might expect a high correlation between behavioral measures. Indeed, we observed an extremely high correlation between spatial and imitation compatibility effects ($r = 0.92$, $P < 0.001$; Fig. 3B). A similar correlation did not exist for accuracy effects, likely due to lack of variability in percent errors across subjects.

Imaging Data

Task activation

The typical subtraction analysis resulted in extremely similar patterns of activation for spatial and imitative cues. The Incompatible > Compatible contrast for both cue types revealed activation of bilateral superior parietal lobule (SPL), dorsal premotor cortex (PMd), and presupplementary motor (pre-SMA) area, as well as insula and cerebellum. To identify any activation specific to one or the other cue type, we examined the cue type \times compatibility interaction [(ImI - ImC) - (SpI - SpC) and (SpI - SpC) - (ImI - ImC)]. Paralleling the similarity between compatibility effects, there were no areas showing significant interactions, even uncorrected or at a more liberal

threshold ($z > 1.7$, corrected). The overlay conjunction illustrates the significant overlap between compatibility effects for the two cue types in all activated regions (Fig. 4A and Table I).

To rule out the possibility that imitative and spatial cues were being processed identically (for example, that the hand in the background or the similar trajectory of both cue types biased subjects toward mental imagery of finger movement even when stimuli depicted dot movement) we contrasted the imitation and spatial cues (collapsed across compatibility). In addition to more robust activation in visual areas, there was increased activation in fronto-parietal areas known to activate during imitation (ventral premotor cortex and superior parietal lobule), [Iacoboni et al., 1999] in imitation blocks compared to spatial blocks ($z > 3.1$, uncorrected; Fig. 4B). No areas showed significantly more activation for spatial than imitative cues.

Functional connectivity

In contrast to the subtraction analysis, functional connectivity results revealed striking differences between cue types. The functional connectivity of the network seed was

TABLE I. Peaks of activity for Incompatible > Compatible for each cue type

Anatomical region	Incompatible > Compatible							
	Imitation				Spatial			
	Z	x	y	z	Z	x	y	z
R LOC/SPL	4.72	16	-64	58	5	16	-66	58
L LOC/SPL	4.97	-16	-62	64	3.97	-24	-60	56
R PMd	5.01	32	0	62	4.96	24	0	56
L PMd	4.49	-24	-10	50	4.78	-26	-4	52
R Insula	4.54	34	16	4	4.71	42	18	2
L Insula	4.16	-32	14	2	4.61	-32	14	-10
R PMv	4.14 ^a	56	10	38	4.28	52	8	30
R IPL	4.2	42	-46	36	4.66	40	-38	50
preSMA	4.39	-8	16	42	4.36	4	18	52
ACC	4.23	12	22	24	4.33	8	22	32
R cerebellum	4.32	28	-56	-34	4.48	44	-56	-30
L cerebellum	4.31	-28	-60	-32	4.33	-32	-46	46

^aDoes not survive correction for multiple comparisons. Anatomical regions of peak voxel within cluster assigned using Harvard-Oxford Cortical and Subcortical Probabilistic Structural Atlases. L and R refer to left and right hemispheres; x, y, and z refer to the MNI coordinates corresponding to the left-right, anterior-posterior, and inferior-superior axes, respectively; Z refers to the highest Z score within a cluster. PMv = ventral premotor; LOC = lateral occipital complex; SPL = superior parietal lobe; IPL = inferior parietal lobe; SMA = supplementary motor area; ACC = anterior cingulate cortex.

modulated by compatibility differentially for spatial and imitative cues. For imitative cues, functional connectivity between the network seed and bilateral subcortical structures (thalamus, caudate, and cerebellum), as well as middle frontal gyrus (MFG) and precuneus, was greater for incompatible than compatible trials (Table II). That is, when subjects responded to biological cues activity in these areas was more synchronized with the network seed during incompatible blocks than compatible blocks.

The spatial cues showed a markedly different pattern than imitative cues, both in location and direction of context-dependent functional connectivity. The network seed had greater functional connectivity with extrastriate visual cortex (primarily in V2, according to the Jülich probabilistic histologic atlas [Eickhoff et al., 2007]) during compatible compared to incompatible blocks. No other regions showed context-dependent differences in functional connectivity for spatial cues (Table II). Direct comparison of functional connectivity for spatial and imitative cues confirms the dissociation, with significant differences between cue type observed in left extrastriate visual cortex, right anterior thalamus, and right precuneus (see Fig. 5).

Comparisons with baseline functional connectivity suggest that when cues were imitative the observed differences in connectivity for compatible vs. incompatible blocks were driven by increased functional connectivity compared to baseline in the incompatible condition as well as

decreased connectivity in the compatible condition compared to baseline; the reverse was true for spatial cues (Fig. 5, middle column bar graphs). None of the control seeds showed a similar pattern of compatibility modulated functional connectivity, nor did the composite control seed average resemble the task-related seed results.

A post-hoc ROI analysis performed on these regions to determine whether the absence of a difference in magnitude of activation between compatible and incompatible blocks was due to lack of sensitivity or a true absence of compatibility effects suggested the former. In the thalamus, a cue type (spatial, imitation) × compatibility (compatible, incompatible) ANOVA revealed a main effect of compatibility, with higher activation during incompatible than during compatible blocks. In left extrastriate cortex, where functional connectivity with the network seed was greater during compatible than incompatible blocks, there was also a main effect of compatibility, but this was due to higher activation during compatible blocks than incompatible blocks (opposite to the pattern in the thalamus). There was also a main effect of cue type in extrastriate cortex, with more activation during imitative compared to spatial cues. In the precuneus there were no significant effects. Importantly, there was no cue type × compatibility interaction in any region, indicating that in contrast to the functional connectivity results, compatibility effects are identical for spatial and imitative cues in all of these regions when considering activation magnitude (Fig. 5, right column bar graphs).

TABLE II. Peaks for significant PPI effects for each cue type, showing regions where functional connectivity with the network seed is significantly different during compatible and incompatible blocks

Anatomical region	Imitation PPI			
	Z	x	y	z
<i>Incompatible > Compatible</i>				
Thalamus ^a	4.46	4	-4	6
Precuneus ^a	4.28	4	-72	48
R cerebellum	4.28	26	-84	-32
L cerebellum	4.34	-30	-64	-42
R MFG	4.04	50	24	34
L MFG	4.96	-30	30	52
L Temp-Occ Fusiform	4.23	-36	44	-12
<i>Compatible > Incompatible</i>				
None				
Spatial PPI				
<i>Incompatible > Compatible</i>				
None				
<i>Compatible > Incompatible</i>				
Occipital (V2) ^a	5.13	-8	-94	18

^aRegions where PPI effects are significantly different when directly compared between imitative and spatial cues (See Fig. 5).

DISCUSSION

We aimed to examine the neural mechanisms involved in overcoming automatic responses induced by spatially compatible and imitative stimuli. To do this we used two stimulus–response mapping tasks that were identical except for the presence or absence of biological motion. The similarity between the two tasks was made possible by the use of simplistic actions for the imitative stimuli. While the imitative stimuli are somewhat removed from real world imitation, they allowed us to compare imitative and spatial cues in a well-controlled task in which inferences regarding differences can be attributed unequivocally to the presence of action observation.

We observed identical patterns of activation for incompatible compared to compatible responses, as well as similar reaction time profiles, regardless of whether stimuli contained biological or nonbiological cues. To determine if differences between imitation and spatial compatibility were reflected instead in functional connectivity, we examined whether this shared network interacted differentially with other brain regions. This revealed markedly different patterns of functional connectivity for the two cue types, consistent with previous behavioral studies suggesting that automatic imitation and spatial compatibility represent dissociable processes [Brass et al., 2000; Catmur and Heyes, 2010; Press et al., 2008].

Within each cue type, both compatible and incompatible blocks consisted of identical motor responses and stimuli such that differences in activation between incompatible and compatible mappings should not be due to low level perceptual or motor processes. Instead, they should reflect increased demands on visuomotor integration systems: During incompatible mappings, the rule-based response conflicts with the automatically activated compatible response, whereas this conflict is absent for compatible mappings [Eimer et al., 1995; Stürmer and Leuthold, 2003]. As a result, compared to compatible mappings, incompatible mappings require: (1) increased reliance on the rule-based mapping and/or (2) decreased susceptibility to the automatically activated response [Kornblum et al., 1990].

Comparison of incompatible and compatible mappings for both cue types revealed activation of a network similar to previous studies of spatial compatibility [Dassonville et al., 2001; Iacoboni et al., 1996, 1998; Matsumoto et al., 2004; Wager et al., 2005]. Activation was detected in bilateral PMd, SPL, preSMA, cerebellum and insula, all areas known to be involved in planning and execution of motor responses to sensory stimuli [Andersen and Cui, 2009; Iacoboni et al., 1996, 1998; Kurata et al., 2000; Nachev et al., 2008; Passingham, 1993; Picard and Strick, 2001; Sakai et al., 1999]. Furthermore, a similar parieto-prefrontal network is recruited in motor tasks requiring responses to spatial [Iacoboni et al., 1996, 1998] and nonspatial cues [Grafton et al., 1998; Kurata et al., 2000], as well as both visual [Grafton et al., 1998; Iacoboni et al., 1998] and auditory [Iacoboni et al., 1998; Kurata et al., 2000] cues,

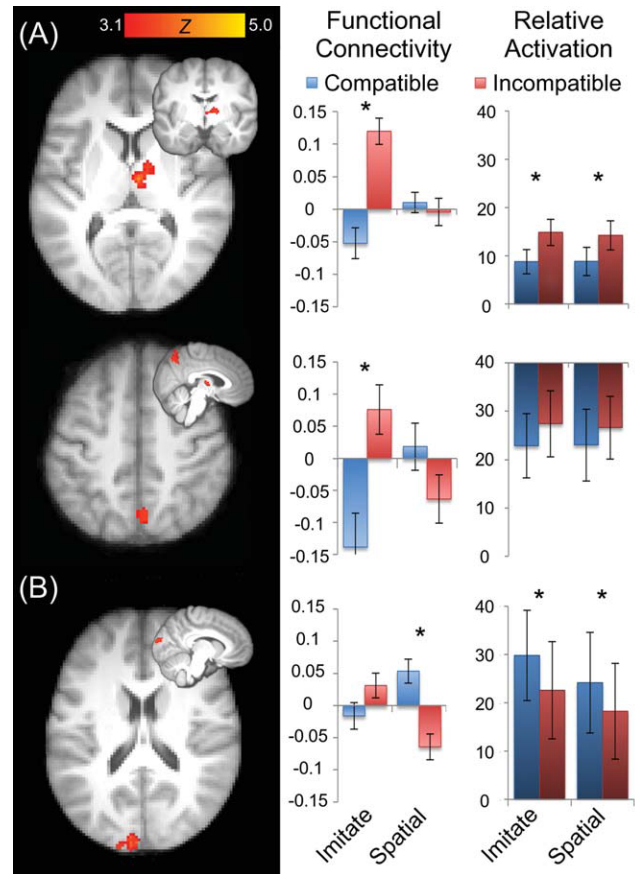


Figure 5.

PPI analysis results. Regions with significantly different PPI effects for imitation and spatial cues. Only those regions that also reach threshold for the individual spatial or imitation PPIs are shown. **(A)** Thalamus and precuneus regions have higher functional connectivity with the network seed during incompatible blocks than during compatible blocks only for imitative cues. **(B)** Occipital cortex region has higher functional connectivity with the network seed during compatible blocks than incompatible blocks only for spatial cues. There were no regions showing similar PPI effects for the two cue types. Mean parameter estimates for the depicted region from post-hoc PPIs (middle column) indicate changes in functional connectivity for compatible and incompatible blocks compared to baseline (error bars are standard error of the mean). Mean parameter estimates from the same regions from post-hoc ROI analysis (right column) depict activation levels for each condition vs. baseline. Significant compatibility effects are indicated with a star (derived from whole-brain PPI for each cue type for functional connectivity graphs; from ROI analysis for relative activation graphs). [Color figure can be viewed in the online issue, which is available at wileyonlinelibrary.com.]

suggesting that this set of coactivated regions is involved in sensorimotor mapping regardless of the input modality or spatial relationship between stimuli and responses. Thus, in the present task similar activation of this network for incompatible mappings for both spatial and imitative cues is consistent with increased demands on a general sensorimotor integration process when the correct incompatible response conflicts with the automatically activated compatible response.

Because a general mechanism for arbitrary stimulus–response mapping is not surprising in the context of the previous work described above, we did expect to observe some overlap in activation for imitative and spatial compatibility effects. However, we also expected differences in the compatibility effects reflecting distinct mechanisms for inhibition of the automatically activated compatible response for imitative and spatial cues [Brass et al., 2009; Catmur and Heyes, 2010], which were not observed. This could be taken to indicate that a single shared process underlies automatic activation and the subsequent inhibition of compatible responses for both stimulus types (supporting the hypothesis that imitation is only a special form of spatial compatibility). For example, a common inhibitory mechanism involving the insula [Nee et al., 2007] and/or PMd [Koski et al., 2005; Praamstra et al., 1999] might explain the identical activation patterns observed. However, we examined the alternative possibility that differences in processing of the two cue types might be reflected in functional connectivity of brain areas showing similar levels of activation [Garraux et al., 2005]. Indeed, this approach revealed that the set of areas showing identical compatibility effects for both cue types had strikingly different patterns of functional connectivity for biological and nonbiological stimuli.

When cues were nonbiological, the network seed exhibited stronger functional connectivity to left visual cortex during compatible blocks than during incompatible blocks. Based on comparisons with functional connectivity at baseline, this difference stemmed both from an increase in functional connectivity during compatible blocks as well as a decrease from resting levels of functional connectivity during incompatible blocks. Decreased connectivity between the network seed and visual cortex may serve to decrease sensitivity to perceptual inputs for incompatible blocks when overlearned visuomotor associations cause automatic activation of the compatible (that is, incorrect) response. Conversely, increased connectivity with visual cortex during compatible trials may reflect increased sensitivity to visual inputs so that the efficient visually driven response has a greater influence on responding. Thus, given that the network seed regions are typically associated with motor planning and response selection, increased functional connectivity of this network with early visual cortex likely reflects an increase in coupling between perception and action when this is beneficial (compatible blocks) and a decrease in perception–action coupling when direct translation interferes with the correct response (incompatible blocks).

In this context, the opposite pattern of functional connectivity for imitative cues—greater connectivity during incompatible than compatible blocks—might reflect a mechanism by which increased interactions serve to decouple perception and action, such that action is driven by internal rules rather than external stimuli during incompatible responding. This pattern of compatibility modulated connectivity specific to the imitation task was observed between the network seed and the right anterior thalamus and precuneus.

A role for the thalamus in decoupling action and perception is supported by reports showing that lesions confined to the thalamus can cause automatic imitative behavior [De Renzi et al., 1996] or utilization behavior [Eslinger et al., 1991; Hashimoto et al., 1995]. These behaviors, in which action is inappropriately driven by environmental cues, can both be conceptualized as forms of excessive perception–action coupling. Similarly, it has recently been shown that inactivation of motor thalamic nuclei cause decreased ability to overcome an automatic saccade toward a visual stimulus and perform a saccade in the opposite direction [Kunimatsu and Tanaka, 2010]. Finally, Guillery and Sherman [Guillery and Sherman, 2011; Sherman and Guillery, 2006] have pointed out that thalamic afferents virtually always have branches delivering the same sensory information to motor areas of the brain, and propose that a role for the thalamus should be considered when examining the close relationship between perception and action.

The precuneus is also frequently involved in tasks requiring visuomotor integration and is important for planning and execution of visually guided movements [Cavanna and Trimble, 2006; Connolly et al., 2003; Ferraina et al., 2001]. Indeed, evidence that the precuneus represents motor goals in multiple coordinate frames (eye-centered, body-centered) suggests it may represent an intermediate stage in transforming perceptual inputs to motor outputs [McGuire and Sabes, 2009]. Thus, the similar connectivity changes between precuneus and thalamus and the set of areas showing compatibility effects during the imitative and spatial tasks have most likely similar functional significance, with increased connectivity serving to decrease perception–action coupling allowing rule-driven stimulus–response transformations to dictate behavior.

This observation of distinct functional connectivity for spatial and imitative cues indicates that overcoming spatially compatible and imitative responses have different underlying neural mechanisms, and is consistent with behavioral studies showing a dissociation between the two tasks [Brass et al., 2000; Catmur and Heyes, 2010; Press et al., 2008]. However this dissociation is not reflected in behavioral compatibility effects in our study (in fact, they were highly correlated), which instead mirror the similarities between activation patterns. This suggests the possibility that behavioral measures may reflect some markers of neural activity more than others (in our dataset,

activation levels more than connectivity). Studies with multiple markers of brain activity are relatively recent, and clearly more data are needed to test this hypothesis.

A dissociation between cue type compatibility effects was also absent in anterior medial frontal and temporoparietal regions, which were previously implicated in control of automatic imitation [Brass et al., 2005, 2009; Spengler et al., 2009, 2010]. Although there was increased activation in the ACC similar to that previously described [Brass et al., 2009], this was not unique to imitation making it unlikely to reflect a specialized imitation control mechanism related to intention attribution as previously hypothesized [Brass et al., 2009; Spengler et al., 2009, 2010]. Instead, we propose that differences in functional connectivity when cues are imitative and spatial may reflect nuanced mechanisms for controlling perception–action coupling depending on the precise nature of the conflict that must be resolved during visuomotor mapping. Whether the different connectivity profiles reflect distinct top-down control mechanisms or instead a mechanism for switching between different perception–action linkages [Hommel, 2009] remains unclear. Further work will be required to determine the precise role of these changing functional interactions.

More generally, divergent patterns of context-dependent functional connectivity for imitative versus spatial cues provide a striking example of a case in which the same network can be similarly activated (as evidenced by identical compatibility effects for the two cue types in the whole brain and ROI analyses), but reflect different processing mechanisms based on functional interactions between the recruited brain regions. We believe that the relative scarcity of data indicating that different processing mechanisms can be coded as differences in network interactions in absence of any regional activation differences is likely a result of common neuroscience practice rather than it being an unusual mechanism of neural coding. Seed-based correlation methods require that a seed is selected, and this is almost always done based on activation differences (in either the same study or previous work). However, in the relatively few examples in which the seeds for functional connectivity analyses were chosen based on similar levels of activation, distinct patterns of context-dependent functional connectivity have also been observed [Garraux et al., 2005; Neufang et al., 2008; Sakai and Passingham, 2006; Stephan et al., 2003]. The present study extends these previous findings of similar activation with different connectivity beyond individual regions of activation to an entire task network—the two tasks relied on a single sensorimotor network with no regional differences in activation across the whole brain, but this network accomplished the task through differential interactions between brain regions.

Another notable feature of the present results is the striking overlap in patterns of functional connectivity of multiple seeds. Frequently functional connectivity analyses focus on one or two regions from a task network in order

to disentangle the contribution of different areas to the cognitive process of interest. In a situation where a broader network is recruited, this requires the seeds of interest be chosen from the network based on a priori hypotheses or assumptions. Here, we used an alternative approach to examine patterns of functional connectivity that were shared between all task-related seeds after noticing that multiple seeds had prominent similarities in their pattern of functional connectivity. This strategy revealed regions in which changes in functional connectivity distinguished between cue type, suggesting that functional connectivity of an entire distributed network, rather than an individual component of this network, may reflect different processing mechanisms. Taken together, this dataset provides a good example of how both functional specialization and network interactions, or “functional segregation and integration,” can be flexibly combined for efficient neural coding, supporting current models of brain organization [Bressler and Kelso, 2001; Friston, 2009].

REFERENCES

- Andersen RA, Cui H (2009): Intention, action planning, and decision making in parietal-frontal circuits. *Neuron* 63:568–583.
- Banks SJ, Eddy KT, Angstadt M, Nathan PJ, Phan KL (2007): Amygdala-Frontal connectivity during emotion regulation. *Soc Cogn Affect Neurosci* 2:303–312.
- Beckmann CF, Jenkinson M, Smith SM (2003): General multilevel linear modeling for group analysis in FMRI. *Neuroimage* 20:1052–1063.
- Brass M, Bekkering H, Wohlschläger A, Prinz W (2000): Compatibility between observed and executed finger movements: Comparing symbolic, spatial, and imitative cues. *Brain Cogn* 44:124–143.
- Brass M, Bekkering H, Prinz W (2001a): Movement observation affects movement execution in a simple response task. *Acta Psychol (Amst)* 106:3–22.
- Brass M, Zysset S, von Cramon DY (2001b): The inhibition of imitative response tendencies. *Neuroimage* 14:1416–1423.
- Brass M, Derrfuss J, Matthes-von Cramon G, von Cramon DY (2003): Imitative response tendencies in patients with frontal brain lesions. *Neuropsychologia* 17:265–271.
- Brass M, Derrfuss J, von Cramon DY (2005): The inhibition of imitative and overlearned responses: A functional double dissociation. *Neuropsychologia* 43:89–98.
- Brass M, Ruby P, Spengler S (2009): Inhibition of imitative behavior and social cognition. *Philos Trans R Soc Lond B Biol Sci* 364:2359–2367.
- Bressler SL, Kelso JA (2001): Cortical coordination dynamics and cognition. *Trends Cogn Sci* 5:26–36.
- Broca P (1961): Remarques sur le siege de la faculte du langage articule, suivies d’une observation d’aphemie (perte de la parole). *Bull Soc Anat Paris* 6:330–367.
- Brodman K (1909): Vergleichende Lokalisation der Grosshirnrinde in ihren Prinzipien dargestellt auf Grund des Zellaufbaus. Leipzig: JA Barth.
- Catmur C, Heyes C (2011): Time course analyses confirm independence of imitative and spatial compatibility. *J Exp Psychol Hum Percept Perform* 37:409–421.

- Cavanna AE, Trimble MR (2006): The precuneus: A review of its functional anatomy and behavioural correlates. *Brain* 129:564–583.
- Chartrand TL, Bargh JA (1999): The chameleon effect: The perception-behavior link and social interaction. *J Pers Soc Psychol* 76:893–910.
- Connolly JD, Andersen RA, Goodale MA (2003): FMRI evidence for a “parietal reach region” in the human brain. *Exp Brain Res* 153:140–145.
- Dassonville P, Lewis SM, Zhu XH, Ugurbil K, Kim SG, Ashe J (2001): The effect of stimulus-response compatibility on cortical motor activation. *Neuroimage* 13:1–14.
- De Renzi E, Cavalleri F, Facchini S (1996): Imitation and utilization behavior. *J Neurol Neurosurg Psychiatry* 61:396–400.
- di Pellegrino G, Fadiga L, Fogassi L, Gallese V, Rizzolatti G (1992): Understanding motor events: A neurophysiological study. *Exp Brain Res* 91:176–180.
- Egner T, Hirsch J (2005): Cognitive control mechanisms resolve conflict through cortical amplification of task-relevant information. *Nat Neurosci* 8:1784–1790.
- Egner T, Delano M, Hirsch J (2007): Separate conflict-specific cognitive control mechanisms in the human brain. *Neuroimage* 35:940–948.
- Eickhoff SB, Paus T, Caspers S, Grosbras MH, Evans AC, Zilles K, Amunts K (2007): Assignment of functional activations to probabilistic cytoarchitectonic areas revisited. *Neuroimage* 36:511–521.
- Eimer M, Hommel B, Prinz W (1995): S-R compatibility and response selection. *Acta Psychol (Amst)* 90:301–313.
- Eslinger PJ, Warner GC, Grattan LM, Easton JD (1991): “Frontal lobe” utilization behavior associated with paramedian thalamic infarction. *Neurology* 41:450–452.
- Ferraina S, Battaglia-Mayer A, Genovesio A, Marconi B, Onorati P, Caminiti R (2001): Early coding of visuomanual coordination during reaching in parietal area pec. *J Neurophysiol* 85:462–467.
- Friston KJ (2002): Beyond phrenology: What can neuroimaging tell us about distributed circuitry? *Annu Rev Neurosci* 25:221–250.
- Friston KJ (2009): Modalities, modes, and models in functional neuroimaging. *Science* 326:399–403.
- Friston KJ, Buechel C, Fink GR, Morris J, Rolls E, Dolan RJ (1997): Psychophysiological and modulatory interactions in neuroimaging. *Neuroimage* 6:218–229.
- Gallese V, Fadiga L, Fogassi L, Rizzolatti G (1996): Action recognition in the premotor cortex. *Brain* 119:593–609.
- Garraux G, McKinney C, Wu T, Kansaku K, Nolte G, Hallett M (2005): Shared brain areas but not functional connections controlling movement timing and order. *J Neurosci* 25:5290–5297.
- Grafton ST, Fagg AH, Arbib MA (1998): Dorsal premotor cortex and conditional movement selection: A PET functional mapping study. *J Neurophysiol* 79:1092–1097.
- Guillery RW, Sherman SM (2011): Branched thalamic afferents: What are the messages that they relay to the cortex? *Brain Res Rev* 66:205–219.
- Hashimoto R, Yoshida M, Tanaka Y (1995): Utilization behavior after right thalamic infarction. *Eur Neurol* 35:58–62.
- Hommel B (2009): Action control according to TEC (theory of event coding). *Psychol Res* 73:512–526.
- Iacoboni M, Woods RP, Mazziotta JC (1996): Brain-behavior relationships: Evidence from practice effects in spatial stimulus-response compatibility. *J Neurophysiol* 76:321–331.
- Iacoboni M, Woods RP, Mazziotta JC (1998): Bimodal (auditory and visual) left frontoparietal circuitry for sensorimotor integration and sensorimotor learning. *Brain* 121:2135–2143.
- Iacoboni M, Woods RP, Brass M, Bekkering H, Mazziotta JC, Rizzolatti G (1999): Cortical mechanisms of human imitation. *Science* 286:2526–2528.
- Iacoboni M, Koski LM, Brass M, Bekkering H, Woods RP, Dubeau MC, Mazziotta JC, Rizzolatti G (2001): Reafferent copies of imitated actions in the right superior temporal cortex. *Proc Natl Acad Sci USA* 98:13995–13999.
- Jenkinson M, Smith S (2001): A global optimization method for robust affine registration of brain images. *Med Image Anal* 5:143–156.
- Jenkinson M, Bannister P, Brady M, Smith S (2002): Improved optimization for the robust and accurate linear registration and motion correction of brain images. *Neuroimage* 17:825–841.
- Kornblum S, Hasbroucq T, Osman A (1990): Dimensional overlap: Cognitive basis for stimulus-response compatibility—A model and taxonomy. *Psychol Rev* 97:253–270.
- Koski L, Iacoboni M, Dubeau MC, Woods RP, Mazziotta JC (2003): Modulation of cortical activity during different imitative behaviors. *J Neurophysiol* 89:460–471.
- Koski L, Molnar-Szakacs I, Iacoboni M (2005): Exploring the contributions of premotor and parietal cortex to spatial compatibility using image-guided TMS. *Neuroimage* 24:296–305.
- Kunimatsu J, Tanaka M (2010): Roles of the primate motor thalamus in the generation of antisaccades. *J Neurosci* 30:5108–5117.
- Kurata K, Tsuji T, Naraki S, Seino M, Abe Y (2000): Activation of the dorsal premotor cortex and pre-supplementary motor area of humans during an auditory conditional motor task. *J Neurophysiol* 84:1667–1672.
- Lhermitte F, Pillon B, Serdaru M (1986): Human autonomy and the frontal lobes. Part I: Imitation and utilization behavior: A neuropsychological study of 75 patients. *Ann Neurol* 19:326–334.
- Matsumoto E, Misaki M, Miyauchi S (2004): Neural mechanisms of spatial stimulus-response compatibility: The effect of crossed-hand position. *Exp Brain Res* 158:9–17.
- McGuire LMM, Sabes PN (2009): Sensory transformations and the use of multiple reference frames for reach planning. *Nat Neurosci* 12:1056–1061.
- McIntosh AR, Korostil M (2008): Interpretation of neuroimaging data based on network concepts. *Brain Imaging and Behavior* 2:264–269.
- Meltzoff AN, Moore MK (1977): Imitation of facial and manual gestures by human neonates. *Science* 198:75–78.
- Nachev P, Kennard C, Husain M (2008): Functional role of the supplementary and pre-supplementary motor areas. *Nat Rev Neurosci* 9:856–869.
- Nee DE, Wager TD, Jonides J (2007): Interference resolution: Insights from a meta-analysis of neuroimaging tasks. *Cogn Affect Behav Neurosci* 7:1–17.
- Neufang S, Fink GR, Herpertz-Dahlmann B, Willmes K, Konrad K (2008): Developmental changes in neural activation and psychophysiological interaction patterns of brain regions associated with interference control and time perception. *Neuroimage* 43:399–409.
- Niedenthal PM, Barsalou LW, Winkielman P, Krauth-Gruber S, Ric F (2005): Embodiment in attitudes, social perception, and emotion. *Pers Soc Psychol Rev* 9:184–211.

- Passingham RE (1993): *The Frontal Lobes and Voluntary Action*. New York: Oxford University Press.
- Penfield W, Boldrey E (1937): Somatic motor and sensory representation in the cerebral cortex of man as studied by electrical stimulation. *Brain* 60:389.
- Picard N, Strick PL (2001): Imaging the premotor areas. *Curr Opin Neurobiol* 11:663–672.
- Praamstra P, Kleine BU, Schnitzler A (1999): Magnetic stimulation of the dorsal premotor cortex modulates the simon effect. *Neuroreport* 10:3671–3674.
- Press C, Bird G, Walsh E, Heyes C (2008): Automatic imitation of intransitive actions. *Brain Cogn* 67:44–50.
- Rogers SJ, Williams JHG (2006): Imitation in Autism: Findings and controversies. In: Rogers SJ, Williams JHG, editors. *Imitation and the Social Mind: Autism and Typical Development*. New York, NY: Guilford Press. pp277–310.
- Sakai K, Passingham RE (2006): Prefrontal set activity predicts rule-specific neural processing during subsequent cognitive performance. *J Neurosci* 26:1211–1218.
- Sakai K, Hikosaka O, Miyauchi S, Sasaki Y, Fujimaki N, Pütz B (1999): Presupplementary motor area activation during sequence learning reflects visuo-motor association. *J Neurosci* 19:RC1.
- Sherman SM, Guillery RW (2006): *Exploring the Thalamus and its Role in Cortical Function*. Cambridge: MIT Press.
- Smith SM, Jenkinson M, Woolrich MW, Beckmann CF, Behrens TE, Johansen-Berg H, Bannister PR, De Luca M, Drobnjak I, Flitney DE, Niazy RK, Saunders J, Vickers J, Zhang Y, De Stefano N, Brady JM, Matthews PM (2004): Advances in functional and structural MR image analysis and implementation as FSL. *Neuroimage* 23 (Suppl 1):S208–S219.
- Spengler S, von Cramon DY, Brass M (2009): Control of shared representations relies on key processes involved in mental state attribution. *Hum Brain Mapp* 30:3704–3718.
- Spengler S, von Cramon DY, Brass M (2010): Resisting motor mimicry: Control of imitation involves processes central to social cognition in patients with frontal and temporo-parietal lesions. *Soc Neurosci* 5:401–416.
- Stephan KE (2004): On the role of general system theory for functional neuroimaging. *J Anat* 205:443–470.
- Stephan KE, Marshall JC, Friston KJ, Rowe JB, Ritzl A, Zilles K, Fink GR (2003): Lateralized cognitive processes and lateralized task control in the human brain. *Science* 301:384–386.
- Stürmer B, Leuthold H (2003): Control over response priming in visuomotor processing: A lateralized event-related potential study. *Exp Brain Res* 153:35–44.
- Wager TD, Sylvester CY, Lacey SC, Nee DE, Franklin M, Jonides J (2005): Common and unique components of response inhibition revealed by fMRI. *Neuroimage* 27:323–340.
- Williams JH, Waiter GD, Gilchrist A, Perrett DI, Murray AD, Whiten A (2006): Neural mechanisms of imitation and “mirror neuron” functioning in autistic spectrum disorder. *Neuropsychologia* 44:610–621.
- Wolbers T, Schoell ED, Verleger R, Kraft S, McNamara A, Jaskowski P, Büchel C (2006): Changes in connectivity profiles as a mechanism for strategic control over interfering subliminal information. *Cereb Cortex* 16:857–864.
- Woolrich M (2008): Robust group analysis using outlier inference. *Neuroimage* 41:286–301.
- Woolrich MW, Behrens TE, Beckmann CF, Jenkinson M, Smith SM (2004): Multilevel linear modelling for FMRI group analysis using bayesian inference. *Neuroimage* 21:1732–1747.